Development 130, 1339-1351

doi:10.1242/dev.00338


# Endothelin 1-mediated regulation of pharyngeal bone development in zebrafish

**Charles B. Kimmel*, Bonnie Ullmann, Macie Walker, Craig T. Miller† and Justin G. Crump**

Institute of Neuroscience, 1254 University of Oregon, Eugene, OR 97403-1254, USA

†Present address: Department of Developmental Biology, Beckman Center B300, 279 Campus Drive, Stanford University School of Medicine, Stanford, CA 94305-5329, USA

*Author for correspondence (e-mail: kimmel@uoneuro.uoregon.edu)

*Accepted 3 December 2002*

## SUMMARY

**Endothelin 1 (Edn1), a secreted peptide expressed ventrally in the primordia of the zebrafish pharyngeal arches, is required for correct patterning of pharyngeal cartilage development. We have studied mutants and morpholino-injected larvae to examine the role of the Edn1 signal in patterning anterior pharyngeal arch bone development during the first week after fertilization. We observe a remarkable variety of phenotypic changes in dermal bones of the anterior arches after Edn1 reduction, including loss, size reduction and expansion, fusion and shape change. Notably, the changes that occur appear to relate to the level of residual Edn1. Mandibular arch dermal bone fusions occur with severe Edn1 loss. In the dorsal hyoid arch, the dermal opercle bone is usually absent when Edn1 is severely reduced and is usually enlarged when Edn1 is only mildly reduced, suggesting that the same signal can act both positively and negatively in controlling development of a single bone. Position also appears to influence the changes: a branchiostegal ray, a dermal hyoid bone normally ventral to the opercle, can be missing in the same arch where the opercle is enlarged. We propose that Edn1 acts as a morphogen; different levels pattern specific positions, shapes and sizes of bones along the dorso-ventral axis. Changes involving Edn1 may have occurred during actinopterygian evolution to produce the efficient gill-pumping opercular apparatus of teleosts.**

Key words: Endothelin 1, Pharyngeal arch, Branchial arch, Operculum, Dermal bone, Morphogen, Zebrafish

## INTRODUCTION

Teleosts are highly derived ray-finned fish and comprise the most diverse group of vertebrates with over 25,000 extant species. Among the specializations that have led to this remarkable success are adaptations for efficient gill breathing. The gill chamber is supported by a set of dermal bones present along the hyoid or second pharyngeal arch. The most distinctive of these bones is the opercle, a large dorsal fan-shaped bone articulating with the underlying hyomandibula (a cartilage replacement bone) by means of an efficient hinged joint. The opercle is the principal support of the opercular cover and its movements play a major role in respiratory pumping. More ventrally, smaller and more slender branchiostegal rays support the lower part of the pharyngeal cavity in a flexible manner, permitting its expansion and contraction during gill breathing. The set of branchiostegal rays has been recognized for more than 150 years as a meristic series (reviewed by Russell, 1916). As described (Cubbage and Mabee, 1996), adult zebrafish have three branchiostegal rays arranged in a dorsal-ventral (DV) series (*Danio*, Fig. 1A). In teleosts more basal than zebrafish, e.g. herrings and their relatives (*Anchoa*, Fig. 1A), the number of branchiostegal rays is higher. Moreover, Hubbs (Hubbs, 1920) first proposed that the branchiostegal series also includes the opercle, a hypothesis supported by other comparative work (Jollie, 1962; McAllister, 1968; Verraes, 1977; Jarvik, 1980). Indeed, as illustrated by *Anchoa*, the dorsal (opercle) and ventral (branchiostegal ray) elements of the series can be more similar in shape to one another than they are in zebrafish and many other more derived teleosts (see also Hubbs and Hubbs, 1945). Notably there is a prominent DV gradient in size along this series. Evolution within separate teleost lineages also has often resulted in fewer ventral elements (McAllister, 1968), and more specializations between the dorsal and ventral elements of the series.

The differences along the DV axis may have had their origins in the earliest osteichthyans (McAllister, 1968), the clade that includes all living bony fish and the basal extinct paleoniscid shown in Fig. 1B. In an outgroup, acanthodians, the bones of the hyoid series are all branchiostegal-like, similar in shape and size. Therefore, an evolutionary scenario leading to the condition in a derived teleost such as the zebrafish would include (1) the establishment of a DV size gradient within the series, (2) further modification of the dorsal-most element that includes new muscle attachments and its new highly functional joint, and (3) the reduction in the number of ventral elements.

Here we report studies supporting the idea that changes in developmental regulation involving a gene network

controlled by a single conserved intercellular signaling molecule, endothelin 1 (Edn1), may have been involved in all three of these evolutionary changes. Edn1 is expressed in the embryonic pharyngeal arches, where these bones develop.

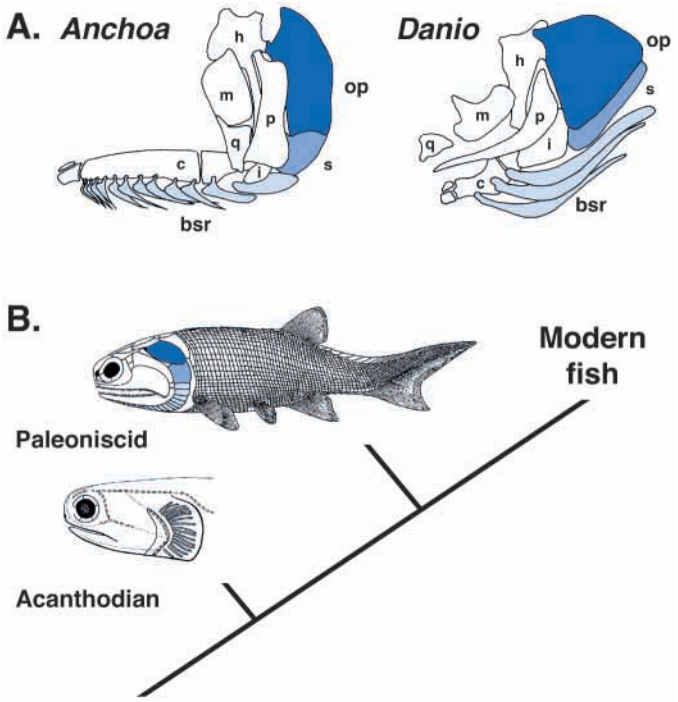


**Fig. 1.** The branchiostegal ray-opercle series of hyoid dermal bones. Left-side views, anterior to the left and dorsal to the top. (A) The series (blue) decorates the hyoid arch, here shown isolated from the rest of the head skeleton, of *Anchoa hepsetus*, a member of the herring family of teleost fish [Clupeidae, from Nelson (Nelson, 1970)], and zebrafish *Danio rerio*, a minnow (Cyprinidae), and considered to be more highly derived with respect to their hyobranchial structures than herrings. The opercle (op) is the dorsalmost bone, branchiostegal rays (bsr) are located ventrally. The branchiostegal rays are generally described as being present as an anterior-posterior series, as makes sense from the adult morphology in *Anchoa*. Primary patterning in zebrafish appears DV, the anterior-posterior orientation seems secondarily derived, reflecting an anterior rotation of the ceratohyal (c) (see Kimmel et al., 2001b) to which the rays attach. Dorsal to the branchiostegal series, and just ventral to the opercle is the subopercle (s), also considered a member of the branchiostegal-opercle meristic series (Hubbs, 1920). There is a prominent size gradient within the series, including all three types of bones. Other bones included in the drawing are the hyomandibula (h), interopercle (i), metapterygium (m), preopercle (p), and quadrate (q). (B) The series in these modern fish may have evolved within the Osteichthyes from a more uniform set of branchiostegal ray-like elements, as represented by the condition in the late-Devonian fossil acanthodian *Homalocantus*. Acanthodians are bony fish sometimes considered to be the osteichthyan sister group (Miles, 1973; Maisey, 1986; Schultze, 1993), their series of hyoid bony spicules might be homologous to the osteichthyan branchiostegal-opercle series (see Janvier, 1996). The DV size gradient was present in the most basal osteichthyans, here represented by the late-Devonian paleoniscid fossil *Moythomasia*, thought to be a representative of the lineage of ray-finned fish (Actinopterygia) that gives rise to teleosts (reviewed by Carroll, 1988). The dorsal-most bone of the series (dark blue) was considered by Hubbs and others to be homologous to the teleost opercle. Drawings adapted from Janvier (Janvier, 1996).

Reduced function of the Edn1-controlled network produces a prominent skeletal phenotype shared among mice, chickens and zebrafish – namely the reduction or loss of specific pharyngeal cartilages (Kurihara et al., 1994; Clouthier et al., 1998; Clouthier et al., 2000; Yanagisawa et al., 1998; Kempf et al., 1998). Prominent among these affected elements is Meckel's cartilage of the embryonic lower (ventral) jaw, the mandible, suggesting that Edn1 plays a key role in pharyngeal skeletal patterning in all jawed vertebrates, the gnathostomes (Miller et al., 2000; Kimmel et al., 2001a). The gene encoding the Edn1 ortholog in zebrafish was first identified in a genetic screen: a single allele was recovered and named *sucker* for the prominent facial phenotype of mutant larvae (Piotrowski et al., 1996). Subsequent work establishes that the mutant phenotype is because of a severe loss of function of the *sucker* (*edn1*) gene (Miller et al., 2000). Phenotypic analyses show that the zebrafish Edn1 network regulates development of ventral pharyngeal cartilages in both the mandibular (first) and hyoid (second) arch, is required for aspects of dorsal cartilage development in the same arches, and is also required for development of the joints normally made between the dorsal and ventral cartilage in both arches (Piotrowski et al., 1996; Kimmel et al., 1998; Miller et al., 2000; Miller and Kimmel, 2001). Edn1 may function generally in gnathostomes to specify skeletal pattern along the DV axis of the pharynx.

How Edn1 plays this DV patterning role, particularly the patterning of ventral cartilage and joint development, is beginning to be unraveled (Miller et al., 2000; Miller et al., 2003). The expression of the *edn1* gene is complex and dynamic. Prominent expression domains located ventrally in the pharyngeal arch primordia correlate with the prominent loss of function phenotype of ventral cartilage reduction. Both ventral epithelium and the ventral mesodermal arch cores express *edn1*; the secreted Edn1 protein probably acts directly on the postmigratory neural crest-derived ectomesenchyme that differentiates into ventral cartilage. Immediate responses in the ventral postmigratory crest to Edn1 signaling include the initiation and/or maintenance of transcription of several developmental regulatory genes, including genes encoding transcription factors such as Goosecoid and Hand2 (dHAND). These genes are also Edn1 targets in the mouse (Clouthier et al., 1998; Clouthier et al., 2000; Thomas et al., 1998; Charité et al., 2001), suggesting broad conservation of aspects of the entire genetic regulatory system among gnathostomes. Expression studies in zebrafish, particularly of the homeobox gene *bapx1* in the mandibular arch, also show that the joints develop, under control of Edn1, from an intermediate region along the DV axis of neural crest-derived mesenchyme that appears remote (but only slightly so) from the ventral Edn1 source. These findings suggest that secreted Edn1 can act at a distance from its source (Miller et al., 2003).

In contrast to the functions of Edn1 in cartilage patterning, its role in development of pharyngeal bones in zebrafish was unknown. Here we describe how reducing Edn1 function affects development of these bones in the young larva, with special focus on the dermal bones of the hyoid arch. The severe loss of function phenotype is dramatic; every bone that is normally present in the pharynx of a 1-week old larva is missing or modified in *edn1* mutants. Dermal bones developing in the mandibular arch are malformed and show polarity

reversals in mutants, consistent with the cartilage phenotypes in this arch. Lowering Edn1 results in an outstanding variety of dermal bone phenotypes in the hyoid arch. The changes involve both the opercle and branchiostegal rays, and include bone loss, expansion, shape change, fusion and probable homeotic transformation. We provide evidence that these remarkably different bone phenotypes result from lowering *edn1* gene function to different levels, and we interpret the results to mean that bone patterning is exquisitely sensitive to the strength of the Edn1 signal. Our data support the hypothesis that Edn1 acts as a morphogen, regulating bone development along the DV axis in a concentration-dependent manner. Changes in, or in responses to, the Edn1 gradient may have underlain evolution of the branchiostegal-opercle series in teleosts and their ancestors.

## MATERIALS AND METHODS

### Animals

Zebrafish of the AB strain were maintained and bred, and embryos reared at 28.5ºC as described (Westerfield, 1995). Developmental times refer to hours or days after fertilization. The mutants, crossed onto the AB background, include *sucker(endothelin1)*$^{tf216b}$ (abbreviated here as *edn1*), *schmerle*$^{tg203e}$ (*she*), *sturgeon*$^{tg419}$ (*stu*), *hoover*$^{tn213}$ and *hoover*$^{b631}$ (*hoo*). The *hoo*$^{b631}$ allele has not been published previously; it fails to complement *hoo*$^{tn213}$, maps to the same locus and mutants phenotypically resemble *hoo*$^{tn213}$ mutants (C. T. M., unpublished). We intercrossed heterozygous carriers for each of the mutations to obtain the homozygous larvae for our analyses; the mutations all produce larval lethality at high penetrance. A translation blocking *edn1* morpholino (*edn1*-MO) was used as described (Miller and Kimmel, 2001).

### Larval skeletal and neuromast staining

Alcian Green was used for cartilage staining in whole fixed larvae as described (Kimmel et al., 1998; Miller et al., 2000), and cartilages dissected and prepared as flat mounts (Kimmel et al., 1998). Developing bone matrix was usually labeled by overnight immersion of live or fixed larvae in 50 μg/ml Calcein (Molecular Probes, Eugene, OR) made in Embryo Medium (Westerfield, 1995), followed by five rinses in Embryo Medium to remove excess dye. For double labeling of bones and neuromasts, the larvae were first vitally stained overnight with 4 μg/ml of Alizarin Red S (Sigma, St Louis, MO), and then rinsed and stained for 10 minutes with 40 μg/ml of DASPEI (Molecular Probes), followed by five rinses. Immunocytochemistry with the zns5 monoclonal antibody (see Johnson and Weston, 1995) was performed as described by Maves et al. (Maves et al., 2002).

### Image acquisition and processing

Bone and neuromast phenotypes in the Calcein or Alizarin Red-DASPEI preparations were scored at a magnification of 50×, with a Leica MZ FLIII stereomicroscope equipped with epifluorescence optics. Higher magnification images were obtained with a Zeiss Pascal confocal microscope: z-series were captured through the pharyngeal regions of interest of larvae mounted at orientations to provide optimal views of the bones. We studied the bones in projection views made from the z-stacks (Zeiss software); generally we processed the images with Adobe PhotoShop to enhance contrast and decrease background. Several of the figures below (e.g. Fig. 2) show black and white negative images (to improve reproduction) of the fluorescent bones in such projections. Alcian Green-labeled flat-mounted cartilages were photographed with differential interference contrast (DIC) optics, using a Zeiss Axiophot microscope (Kimmel et al., 1998).

## RESULTS

### Wild-type pattern of pharyngeal bones and changes in *edn1* mutants

The 74 bones comprising the head skeleton of the mature zebrafish develop at specific locations in a stereotyped sequence of ossification (Cubbage and Mabee, 1996). The rudiments of nine of them are developing in the pharyngeal arches of wild-type larvae one week after fertilization (Fig. 2A). The elements include both dermal and cartilage replacement bones in the first two and the last of the seven arches (see the Fig. 2 legend for their classification).

We observed that all of the cartilage replacement bones of the anterior two arches are invariably absent in *sucker(edn1)*$^{tf216b}$ mutants (*edn1*$^{-}$). The dermal bones are absent or malformed. Below we explore the condition of the dermal bones of the mandibular arch and especially

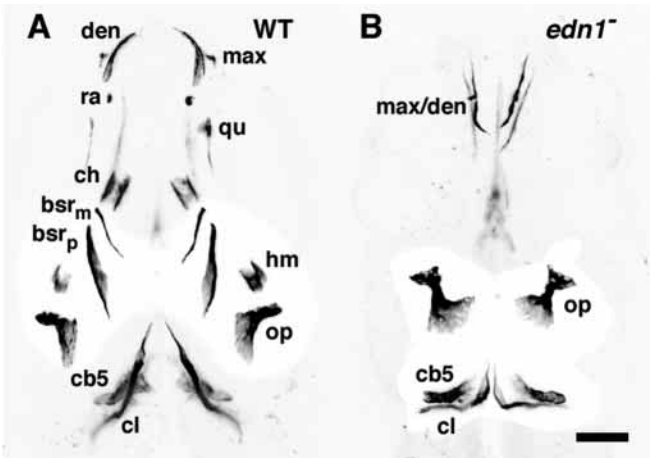


**Fig. 2.** Ossifications in the young wild-type (WT) zebrafish (A) and homozygous *edn1* mutant (B). Ventral views, anterior to the top, of negative images of bones fluorescently labeled with Calcein in larvae at 7-days postfertilization. Ventral bones of the pharyngeal arches are identified (Cubbage and Mabee, 1996) by their labels on the left side, and dorsal bones are labeled on the right side in both panels, all of them are present as bilateral pairs. (A) The wild type first or mandibular arch includes a dorsal and a ventral dermal bone, the maxilla (max) and dentary (den), and a dorsal and a ventral cartilage-replacement bone, the quadrate (qu) and retroarticular (ra). The second or hyoid arch includes a dorsal and two ventral dermal bones, opercle (op), and two branchiostegal rays (bsr$_p$ and bsr$_m$), and dorsal and ventral cartilage replacement bones (very incompletely ossified at this stage), the hyomandibula (hm) and ceratohyal (ch). The most posterior arch includes a cartilage-replacement bone, ceratobranchial 5 (cb5). Overlaying ceratobranchial 5 is the cleithrum (cl), a long dermal bone connecting the posterior skull and the pectoral girdle. Two other craniofacial bones present at this stage lie deeper in the tissue and are not labeled, the parasphenoid and the endopterygoid. (B) Many of the anterior ossifications (in the first two arches) are missing in the *edn1* mutant. Ceratobranchial 5 and the cleithrum are present, shortened and somewhat malformed. In the mandibular arch dermal bones (max/den) are present but severely malformed, an example of the 'wicket' phenotype discussed in the text (see also Fig. 3). In the hyoid arch the opercle is present and its joint region (upper part of the bone) is markedly expanded, a mild example of the 'opercle-gain' phenotype described in the text and other Figures. Scale bar: 100 μm.

the hyoid arch in some detail. Briefly, in the mutant mandibular arch, the maxilla and dentary are fused together, misoriented and misshapen. In the mutant hyoid arch, branchiostegal rays are absent (but see below), and the opercle is either absent or alternatively the opercle is present and enlarged (Fig. 2B).

### The dermal jaw bones

Development of the dermal bones of the mandibular arch (first pharyngeal arch, forming the upper and lower jaws) is severely perturbed when Edn1 is lowered, either as in *edn1* mutants (Fig. 3), or by the translation-blocking *edn1* morpholino (*edn1*-MO). In wild-type larvae, a dentary is positioned superficially to Meckel's cartilage in the lower (ventral) jaw on each side of the midline. It is fan-shaped posteriorly (Fig. 3A) and anteriorly curves (Fig. 3B), deep to the lower lip. At this stage the bilateral dentaries do not yet join together at the anterior midline, but are well separated. The maxilla, anterior and superficial to the pterygoid process of the palatoquadrate cartilage in the upper (dorsal) jaw, is more dorsal-ventrally oriented than the dentary (best seen in the side view in Fig. 3A).

In *edn1* mutants, the mouth is wide open and is extremely malformed. The lower jaw points in the wrong direction. It is reversed in anterior-posterior orientation, such that the lower lip curves posteriorly rather than anteriorly, and is located ventral to the eyes rather than anterior to the eyes as in the wild type. In place of the two bilateral pairs of mandibular arch dermal bones curving anteriorly in the wild type, in the *edn1* mutants or *edn1*-MO-injected larvae we frequently observe a thin, bilateral wicket-shaped single element with a posterior curvature that follows the outline of the mouth, just deep to the lips (Fig. 3C). However, the expressivity of the phenotype varies among individual mutants. Sometimes there are gaps in the bone at the midline and approximately midway along the arms of the wicket (arrows, Fig. 3D,E). We infer from these patterns (and also from phenotypes in *edn1*-MO-injected embryos; see legend to Fig. 3) that the wicket includes the rudiments of both dentaries and maxillas, fused together more or less completely in different individual mutants. The dentary would represent the posterior part of the wicket reversed in anterior-posterior polarity, as suggested from the curvature of the bone and the way it follows the lower lip (as in the wild type). We note that the cartilage phenotypes in the same arch of *edn1* mutants are interpreted similarly: the dorsal cartilages and the remnants of the ventral cartilages are invariably fused to one another, and the anterior-posterior polarity of the ventral cartilage is reversed (Piotrowski et al., 1996; Kimmel et al., 1998) (see Discussion).

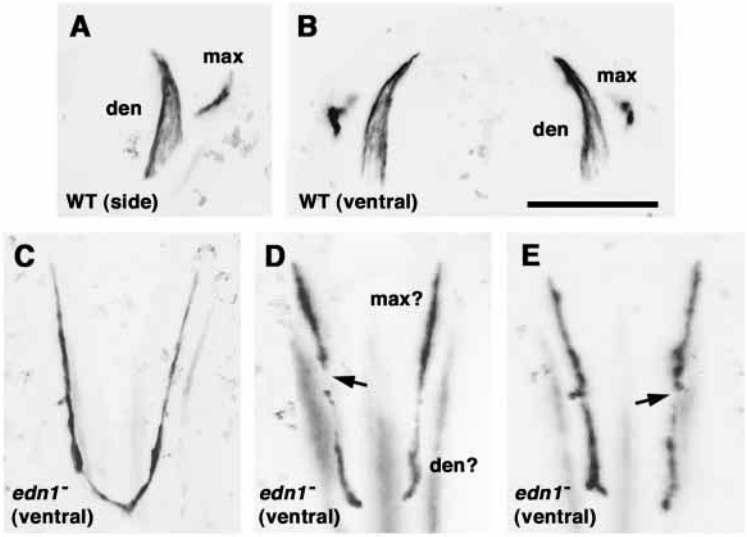


**Fig. 3.** Dermal bones of the mandibular arch and their transformations in *edn1* mutants. Anterior is to the top. The wild-type (WT) maxilla (max) and dentary (den) are shown in right-side view (dorsal to the right) (A) and ventral view (B). (C-E) Three examples of the AP-reversed wicket phenotype in three individual *edn1* mutants, that we interpret to include the malformed bilateral rudiments of the maxillas and dentaries, completely fused (C), or incompletely fused together (D,E) (ventral views, see also Fig. 2 for orientation). The arrows in D and E indicate variably present gaps along the wicket arms. In examples not shown with only mild reduction of Edn1 (as obtained in *sturgeon* mutants or when *edn1*-MO is injected at low levels), the maxilla and dentary are frequently normally shaped, but misoriented: the orientation relates to the change in the shape of the mouth, as in *edn1* mutants. Injected at higher levels, *edn1*-MO yields the wicket phenotype, phenocopying the *edn1* mutants, and a yet more extreme phenotype in which only a small bone fragment is present (data not shown). This remaining element is usually located at an anterior position in the wall of the mouth, suggesting that it is a remnant of the maxilla. Scale bar: 100 μm.

### The opercle loss-gain phenotypes

The second or hyoid arches of the larva 1-week after fertilization include the paired rudiments of two cartilage replacement bones (hm, ch; Fig. 2) and at least two elements of the dermal branchiostegal-opercle series (op, $bsr_p$, and variably at this stage $bsr_m$, Fig. 2). All of the bones are missing in some *edn1* mutants. In others, only a bone fragment is present, located dorsally in the segment, approximately at the normal position of the opercle but much smaller than the wild-type opercle and lacking its characteristic fan shape. In yet other individuals, we could easily recognize an opercle. Curiously and almost invariably in the latter class the opercle was enlarged, usually markedly so (Fig. 4). Such contrasting phenotypes, ranging from complete absence to marked expansion, resulting from the same genetic lesion as we observe for the opercle in *edn1* mutants is unusual. To emphasize the contrast we refer to the opercle loss or reduction as the 'loss' phenotype, and to the opercle expansion as the 'gain' phenotype.

The opercle normally makes an articulating joint with a dorsal hyoid cartilage, the hyosymplectic, and the expansion of the gain opercles in *edn1* mutants invariably involves the bone around this joint region (Fig. 4). The hyosymplectic cartilage is present in *edn1* mutants, although often considerably changed in appearance (Kimmel et al., 1998). DIC imaging of both bone and cartilage together in mutant larvae revealed that the gain opercle makes an enlarged articulation with the cartilage at approximately the correct location (Fig. 4B,D). In contrast, in opercle loss examples that include a bone fragment (i.e. as opposed to opercle loss examples in which the bone is completely missing), the fragment is considerably removed from the cartilage, located superficially in

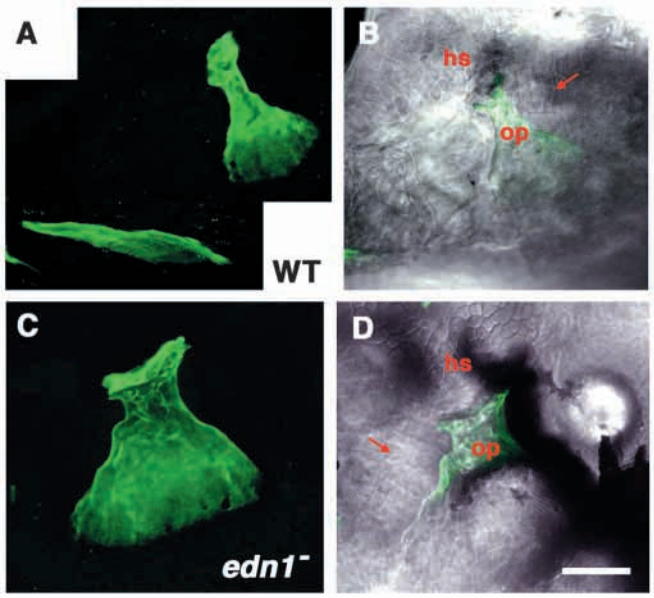


**Fig. 4.** The opercle-gain phenotype in an *edn1* mutant. Left-side views with dorsal to the top at 6-days postfertilization. (A,B) Wild type (WT), (C,D) mutant. (A,C) Projections of the Calcein-labeled bones from z-stacks of sections made by confocal microscopy. (B,D) The same projections are overlaid onto Nomarski differential interference contrast (DIC) images at the plane of focus of the joint made by the opercle (op) with the hyosymplectic cartilage (hs). The opercle (green) at this stage is fan-shaped in the wild type (A). It is similarly shaped but larger in the mutant (B); the joint region (upper) is thicker and the fan is expanded. The DIC views reveal that the opercle-gain joints are made with the hyosymplectic cartilage as in the wild type. In these two panels (B,D) the cells of the hyosymplectic cartilage can be recognized by their characteristic mosaic-tile shapes, and are present just above the opercle. Muscles, identifiable by their striated appearance (arrows), connect with wild type and mutant opercles. Often in the mutants, as here to the left side, ectopic muscles connect to the gain opercle. Scale bar: 50 μm.

dermal mesenchyme just beneath the epidermis (not shown). Another feature of the opercle-gain phenotype revealed by DIC imaging is the frequent presence of ectopic muscles attaching to the enlarged bone. For example, the arrow in Fig. 4D shows a muscle projecting to the blade of the opercle from an anterior location. Normally no such muscle is present.

What accounts for such contrasting loss versus gain opercle phenotypes? The phenotypes seem unlikely to be entirely because of difference in genetic background, because in many cases we see a loss phenotype on one side, and a gain phenotype on the other side of the same mutant larva. Furthermore, the mutant phenotype is not limited to *edn1* mutants. Mutations at three other loci unlinked to *edn1* are all grouped in the same phenotypic class as *edn1* mutants, termed the 'anterior arch class', and some or all of these genes, *schmerle* (*she*), *sturgeon* (*stu*) and *hoover* (*hoo*), may function along the *edn1* genetic pathway (see Piowtroski et al., 1996; Kimmel et al., 1998; Miller and Kimmel, 2001) (C. T. M. and M. W., unpublished). We observed the opercle-gain phenotype in mutants at each of these three other loci, and the opercle-loss phenotype in two of them (Table 1; branchiostegal ray phenotypes are discussed below). Hence, the opercle loss-gain phenotypic pair is not locus-specific.

Study of histological sections (not shown) reveals that all bone in early zebrafish (whether dermal or cartilage replacement) is acellular (reviewed by Beresford, 1996) (see also Parenti, 1986), formed by osteoblasts present along the surfaces of the bone matrix. Dyes such as Calcein or Alizarin Red stain bone matrix but not the osteoblasts, which can be labeled with the monoclonal antibody zns-5 (Johnson and Weston 1995). In early wild-type larvae a prominent cluster of osteoblasts delineates the developing opercle (Fig. 5A, arrow; a cluster of branchiostegal ray osteoblasts is also present at the asterisk). Comparing immunoreactivity in wild type and *stu* (not shown) or *she* mutants revealed two phenotypes, the probable cellular correlates of the loss and gain opercle phenotypes shown by the matrix labeling. Some mutants had a reduction of the size of the opercle osteoblast population (Fig. 5B) and others showed an expansion (Fig. 5C). These findings suggest that the number of embryonic cells recruited as osteoblasts ultimately determines whether a loss or gain opercle phenotype will form.

## The opercle-loss phenotype results from severe reduction of Edn1 and the gain phenotype results from milder reduction

What determines how many opercle osteoblasts develop? The data in Table 1 suggest an explanation for the loss-gain opercle phenotypic pair. We propose that lowering Edn1 function to different levels results in the different phenotypes: we observed only the opercle-gain phenotype in the clutch of *hoo* mutants scored (Table 1) and, because *hoo*$^{-}$ typically has the mildest

**Table 1. Opercle and branchiostegal ray phenotypes in anterior arch mutants**

| | Opercle phenotype | | | Branchiostegal ray phenotype | | |
|---|---|---|---|---|---|---|
| Locus | Wild type | Gain | Loss | Wild type | Gain | Loss |
| *edn1* (clutch 1) | 20 (12%) | 112 (66%) | 38 (22%) | 11 (6%) | 0 (0%) | 159 (94%) |
| *edn1* (clutch 2) | 1 (1%) | 26 (39%) | 40 (61%) | (not scored) | (not scored) | (not scored) |
| *she* | 22 (15%) | 94 (64%) | 33 (22%) | 20 (13%) | 10 (7%) | 120 (80%) |
| *stu* | 34 (24%) | 54 (38%) | 54 (38%) | 22 (15%) | 0 (0%) | 120 (85%) |
| *hoo*$^{tn213}$ | 125 (92%) | 11 (8%) | 0 (0%) | 126 (93%) | 6 (4%) | 4 (3%) |

Homozygous mutants were obtained by crossing heterozygotes that were scored by facial phenotypes and separated from phenotypic wild-type siblings before fixation and bone staining with Calcein. The wild-type phenotype indicates that the element (opercle or branchiostegal ray) appears normal in shape and size. The gain phenotype means any significant expansion (see text). The loss class includes reduction in size, as well as other cases where the element is missing altogether. The two *edn1* examples (separate experiments involving crosses between different individual fish) are quantitatively different, indicating that quantitative comparisons between clutches must be interpreted with caution. Similarly, in other experiments, *stu* mutants had higher fractions of opercle gain phenotypes, comparable with *she* mutants in the table.

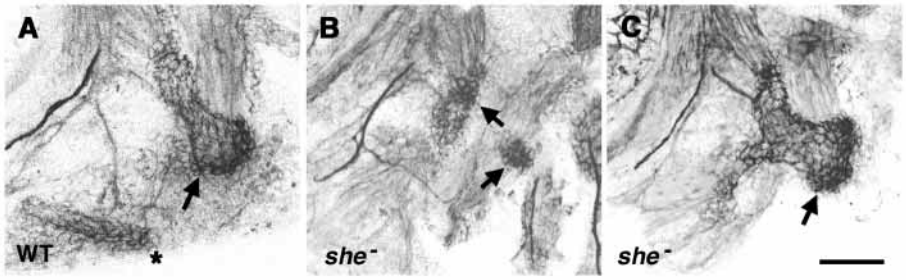


**Fig. 5.** Two classes of opercle osteoblast clusters, expanded and reduced, are present in *she* mutants. Labeling with the zns5 monoclonal antibody in larvae at 88 hours postfertilization. Left-side views with dorsal to the top. The antibody labels both osteoblasts and nerve axons prominently, and muscles lightly. (A) wild type (WT). Osteoblasts envelop the opercle (arrow) and branchiostegal ray (asterisk). The dark lines are nerves. Delicately labeled muscles (at the top) connect separately to the opercle joint region (dilator operculi muscle, left) and blade region (adductor operculi, right). (B) A *she* mutant with a presumed mild opercle-loss phenotype. The branchiostegal ray osteoblast cluster is missing. Two clusters are present (arrows) that seem to correspond to the opercle joint region (upper, identified by its position and its connection with the dilator operculi muscle) and a diminished opercle 'fan' region (lower). A confocal z-series reveals no osteoblasts connect between these two clusters. (C) A *she* mutant with presumed opercle gain. The opercle osteoblast cluster is expanded (arrow), particularly at the joint region. The branchiostegal ray cluster is either missing or possibly is present but fused with the opercle cluster. Muscle connections are approximately normal. Scale bar: 50 μm.

cartilage and facial phenotypes of all of the anterior arch mutants, this result suggests that a mild reduction of Edn1 results in the gain phenotype and a more severe reduction results in the opercle-loss phenotype. We tested this postulate directly by reducing Edn1 function to different levels with *edn1*-MO.

Injecting the *edn1*-MO at moderate or high levels reliably phenocopies in detail the *edn1* mutant defects in gene expression, cartilages and facial appearance (Miller and Kimmel, 2001). When injected at lower levels, the *edn1*-MO phenocopies the facial and cartilage defects of the other anterior arch mutants, resulting in a phenotypic series according to the level of Edn1 reduction, namely *hoo*$^{-}$ (the mildest phenotype, usually obtained with the lowest effective amount of *edn1*-MO) < *stu*$^{-}$ < *she*$^{-}$ < *edn1*$^{-}$ (the most severe, obtained with highest levels) (Miller and Kimmel, 2001).

In the present study, injecting the same morpholino over the same 30-fold concentration range studied previously yielded both the opercle-gain and -loss phenotypes, in proportion to the amount of *edn1*-MO. At the highest useful level we examined (15 ng), *edn1*-MO specifically phenocopies all defects in pharyngeal bones of the *edn1* mutants, with the notable change in several experiments that we observed a higher fraction of opercle-loss phenotypes than we usually observe in *edn1* mutants (85% of injected larvae, $n$=163; compare with Table 1). The increase might be because of differences in genetic background, or might mean that the single available mutant allele, even though severe, is not a null allele (Miller et al., 2000). In the experiment quantified in Fig. 6A-C the opercle-loss phenotype still predominated when the morpholino was injected at 5 ng (A: opercle ranks 1 and 2, totaling 75%). However, at 0.5 ng the opercle-loss phenotype becomes the minority class (C: 19%), and opercles of normal size and with the gain phenotype predominate (respectively in Fig. 6C, wild type; 44%, and opercle gain ranks 3 and 4; 35%). In other experiments with the lower amounts of edn1-MO, as many as 50% of the injected larvae showed the opercle-gain phenotype. Our findings suggest that as predicted, the opercle-gain phenotype results when Edn1 is only mildly reduced, and the loss phenotype results from reduction that is more substantial.

## Opercle, cartilage and lateral line phenotypes co-vary in individual mutants

Pharyngeal cartilage phenotypes in the anterior arch mutants are variable in severity (Piotrowski et al., 1996; Kimmel et al., 1998), as we show here for the pharyngeal bone phenotypes. Do the phenotypes of two skeletal tissues in the same pharyngeal arch vary separately or together? Independence could indicate that Edn1 sources very local to each bone and cartilage might be responsible for patterning. Alternatively, co-variance might indicate that a 'global' Edn1 source within the arch influences both bone and cartilage patterning (see Discussion). We observe that the severity of hyoid cartilage reduction varies as a function of the injected amount of *edn1*-MO (Fig. 6D-F), confirming our previous findings (Miller and Kimmel, 2001). The bone and cartilage data sets were collected from the same larvae, and we kept track of which phenotypes were present on their left and right sides, providing for the correlation analyses shown in Fig. 6G-I. Larvae with the opercle-loss phenotype in one or both hyoid arches, and irrespective of the amount of MO used to obtain these phenotypes, also show very high incidences of severe cartilage loss in the same left or right arches (Fig. 6G). Similarly, arches with the opercle-gain phenotype have the highest incidence of mild cartilage reduction (Fig. 6H), and opercles of normal (wild type) size have the highest incidence of wild type-looking cartilages (Fig. 6I). These data strongly suggest that the two phenotypes co-vary (see also the legend to Fig. 6).

DIC observations during the course of this study revealed that opercular neuromasts, sensory organs of the anterior lateral line system, were frequently missing in anterior arch mutants and in *edn1*-MO-injected larvae. We used two-color methods to score the bone and lateral line phenotypes together in a set of *edn1* mutants (data not shown) and in the set of *edn1*-MO-injected animals used for Fig. 6, and observed strong correlation between the severities of the two phenotypes. Neuromasts occur at stereotyped and largely invariant positions along this region of the pharynx, as well described by Raible and Kruse (Raible and Kruse, 2000). In most uninjected larvae at 6 or 7 days postfertilization the operculum bears two neuromasts located just superficially to the opercle (83%, Table 2; Fig. 7B, OP1, OP2). There is a mild reduction in the number of opercular neuromasts in *edn1*-MO-injected larvae that show the opercle-gain phenotype (74% have both OP neuromasts, Table 2; Fig. 7C). However, only 5% of opercle-loss arches have both opercular neuromasts; rather they have one (60%) or none at all (35%; Fig. 7D). Other neuromasts in the vicinity of

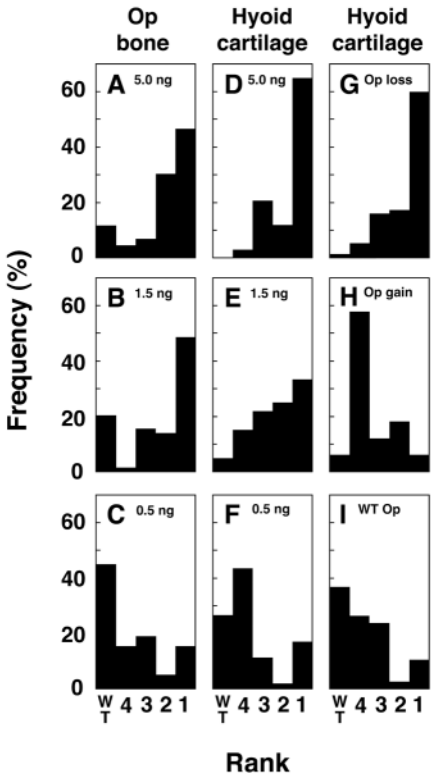


**Fig. 6.** Opercle (A-C) and cartilage (D-F) phenotypes depend on the level of Edn1 reduction in *edn1*-MO-injected larvae, and co-vary in individual hyoid arches (G-I). The MO was injected at 5 ng, 1.5 ng and 0.5 ng. (A-F) Resulting sets of opercle and hyoid cartilage phenotypes, scored independently on both sides of individual larvae, and ranked according to severity. Facial phenotypes (not shown) are as expected (Miller and Kimmel, 2001). The highest levels of *edn1*-MO generally produce the more severe phenotype, resembling *edn1* mutants. Milder facial phenotypes, resembling *hoo*$^{-}$ were observed at the lowest levels. The data are shown as percentages; the number of arches scored (left and right, considered separately) ranged from 33 to 75 for each panel, from a total of 73 larvae (146 sides). (A-C) Opercle ranks are: 1, missing; 2, reduced; 3, mildly expanded (Fig. 8B-F); 4, markedly expanded (Fig. 8G-K); wild type (WT), normal. (D-I) Hyoid cartilage phenotypes were scored according to degree of reduction (we do not observe completely missing cartilages or cartilage expansions), reflecting the spectrum previously shown [Fig. 9 of Kimmel et al. (Kimmel et al., 1998)]: 1 and 2: relatively severe reductions as in typical severe (1) and mild (2) *edn1* mutants; 3, intermediate loss, as in typical *she* mutants; 4, mild loss, as in a typical *stu* mutants; WT, wild type. (G-I) The cartilage ranks shown in animals grouped (independently of the amount of injected MO) by their opercle phenotypes in the same (left or right) hyoid arches. Opercle ranks 1 and 2 (in A) together constitute the opercle-loss group; ranks 3 and 4 together constitute the opercle-gain group, and ranks 3 and 4 together constitute the opercle-gain group. We used Chi-square analysis (data not shown) to test and reject ($P$<0.001) the null hypothesis that severities of cartilage and bone phenotypes vary independently from one another in individual arches. MO, morpholino.

the operculum are also disrupted by compromising Edn1. These other neuromast changes are less frequent than the loss of opercular neuromasts, and include duplications as well as losses (Table 2 includes the scores for one of the more severely affected of these, neuromast M2 located just dorsal and superficial to the opercle-hyosymplectic joint). Similar to the losses of the neuromasts OP1 and OP2, we observed these losses in animals injected with any of the three MO concentrations, and they occurred most frequently in arches also exhibiting the opercle-loss phenotype (e.g. Fig. 7D). Hence, as for the cartilage-bone phenotypes, the severities of neuromast-bone phenotypes often vary together within a single arch.

**Table 2. Correlations between opercle and neuromast phenotypes in *edn1*-MO-injected larvae**

| Class | Number scored | M2 neuromast | Number of OP neuromasts | | |
|---|---|---|---|---|---|
| | | | 2 | 1 | 0 |
| Uninjected | 48 | 48 (100%) | 40 (83%) | 8 (17%) | 0 (0%) |
| Opercle wild type | 44 | 47* (107%) | 27 (90%) | 14 (32%) | 3 (7%) |
| Opercle gain | 35 | 39** (111%) | 26 (74%) | 8 (23%) | 1 (3%) |
| Opercle loss | 86 | 89*** (103%) | 4 (5%) | 52 (60%) | 30 (35%) |

We scored presence or absence of neuromasts in the pharyngeal region (see their labeling in Fig. 7), and (on the same sides of the same larvae) the bone phenotypes. For the table, classes were assigned by phenotype of the opercle, irrespective of amount of injected *edn1*-MO. The frequency distributions for the bone and cartilage phenotypes from the same set of larvae are shown in Fig. 6. As the phenotype varies between the two sides of a single larva, each side of each larva was scored separately, and 'Number scored' refer to sides scored. We used Chi-square analysis (data not shown) to test and reject ($P$<0.001) the null hypothesis that severities of cartilage and OP neuromast phenotypes vary independently from one another in individual arches.

*In three cases, the M2 neuromast was duplicated, resulting in a total of 47.

**In one case, no M2 neuromasts were present; in five cases the M2 neuromast was duplicated, resulting in a grand total of 39.

***In seven cases, no M2 neuromasts were present; in ten cases the M2 neuromast was duplicated, resulting in a grand total of 89.

## DV identity of hyoid bones; homeotic shift between branchiostegal ray and opercle

Similar to the opercle, the hyoid arch branchiostegal ray phenotype also changes according to how severely Edn1 is lowered. At 6 days postfertilization, one and usually two branchiostegal rays are present ventral to the opercle. The posterior and more dorsal ray ($bsr_p$, Fig. 2) appears earlier in development (our work in progress). The branchiostegal rays are often missing (or sometimes one is present but reduced in size) when Edn1 is severely lowered as in *edn1* mutants (Figs 2, 4; Table 1). However, at the minimum, the more dorsal branchiostegal ray develops after only milder Edn1 reduction, as apparently in *she*, *stu* and *hoo* mutants (Table 1) and in larvae injected with the lower amounts of *edn1*-MO (not shown). Formation of a branchiostegal ray is apparently more sensitive to reduction of Edn1 than the opercle; the fraction of branchiostegal loss is always higher than the fraction of opercle loss, and furthermore we never observed the converse situation, i.e. an individual hyoid arch in which the opercle is absent and a branchiostegal ray is present. Rather, in general, the presence of a branchiostegal ray is associated with the opercle-gain phenotype. As for the opercle phenotype, our data suggest that presence or absence of staining of branchiostegal ray bone matrix (e.g. with Calcein) correlates with presence or absence of branchiostegal osteoblasts labeled with zns-5 (Fig. 5).

In cases in which a branchiostegal ray is present, it is abnormally close to the opercle, and is sometimes malformed (Fig. 8). Normally the branchiostegal rays are saber-shaped

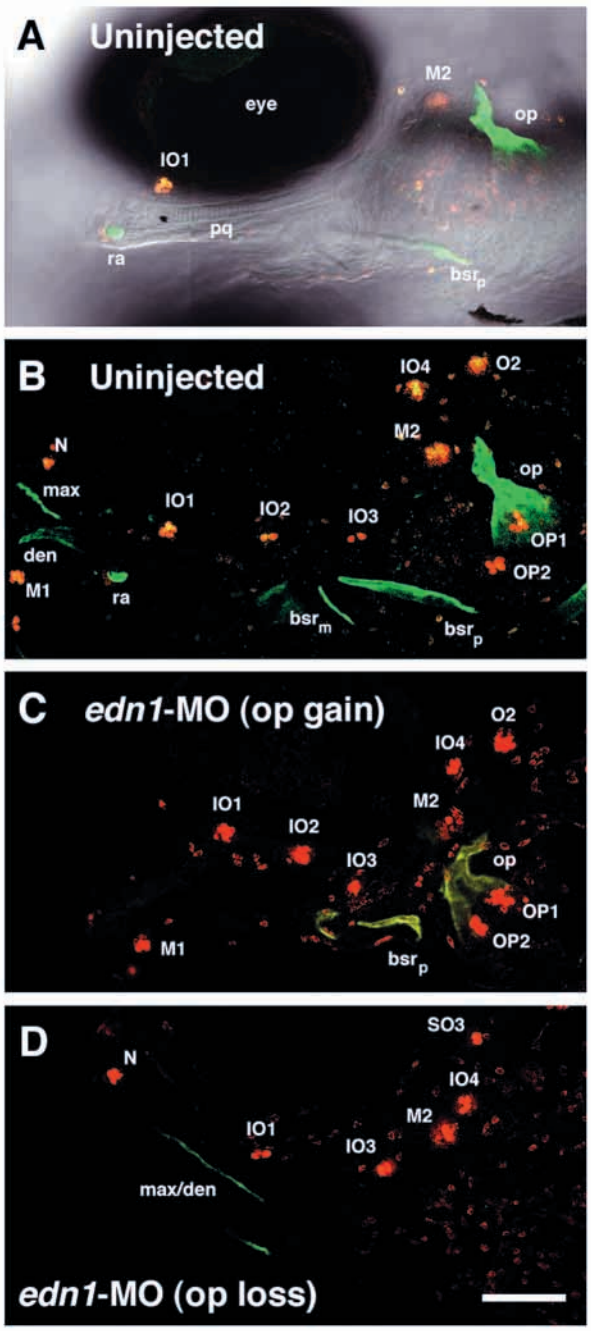


**Fig. 7.** Correlated expressivities of opercle and lateral line neuromast phenotypes in *edn1*-MO-injected larvae (C,D), compared with an uninjected larva (A,B). Left-side views of live larvae, with dorsal to the top and anterior to the left at 6-days post fertilization. (B-D) Confocal *z*-series projections. (A) A single optical section from the image stack in B combining DIC with fluorescence for orientation. The bones are labeled with Calcein (green), and the neuromasts with DASPEI (orange-red). Neuromasts were identified (Raible and Kruse, 2000) and are labeled with upper case letters; other structures are labeled in lower case. (B) The normal neuromast distribution in the uninjected control. (C) An *edn1*-MO-injected larva expressing the opercle-gain phenotype, the branchiostegal ray (bsr) is also malformed. The complete set of neuromasts is present, however IO3 is displaced ventrally and M1 is displaced posteriorly. (D) An *edn1*-MO-injected larva expressing the opercle-loss phenotype. Both the opercle and branchiostegal ray are missing, and the mandibular dermal bones (max/den) resemble the condition in Fig. 3E. The neuromast phenotype in this particular larva is severe; losses include M1, IO2, O2 and the two opercular neuromasts OP1 and OP2. Scale bar: 100 μm. MO, morpholino.

(Fig. 8A). In *she* and *stu* mutants and in *edn1*-MO-injected larvae the branchiostegal ray is often sickle- or scimitar-shaped (Fig. 8G, and extreme case in Fig. 8H), curved with the convexity toward the opercle. Further, in what we term the 'walking stick' phenotype, the opercle and dorsal branchiostegal ray are fused together (Fig. 8B,D,F). Fig. 8K shows a dramatic example of fusion, in which a thin continuous sheet of bone connects the opercle and branchiostegal ray.

The bone fusions suggest that after a mild reduction of Edn1 the opercle and branchiostegal ray are becoming more similar to one another in character – i.e. that we are observing homeosis. Antibody labeling seems to support this interpretation; for example, the osteoblast labeling in the *she* mutant shown in Fig. 5C is suggestive that branchiostegal and opercle osteoblast populations are fused together at the region where the bones attach to the cartilage. Furthermore, the walking stick-branchiostegal ray makes a differentiated joint with the underlying ceratohyal cartilage resembling the joint the opercle makes with the hyosymplectic; a particularly clear example of the branchiostegal joint region bone is shown in Fig. 8F. Normally a branchiostegal ray does not make such a distinctive structure; a blunt end of the bone (uppermost end in Fig. 8A) is simply bound to the ceratohyal by connective tissue.

A rare phenotype in *hoo* mutants is that along with making a joint, the branchiostegal ray enlarges (in 4% of the mutants, Table 1) and strikingly, can take on a fan shape (Fig. 9). Here the dorsal branchiostegal ray might be homeotically transformed, rather completely, into an opercle.

These branchiostegal ray phenotypes, similar to those of the opercle described above, appear to be because of change in Edn1 level, and not because of some other changes associated with mutations at these several loci. To demonstrate this we added back Edn1 into *edn1* mutants, either as human EDN1 protein or as a wild-type zebrafish *edn1* DNA (Miller et al., 2000). Again, at low frequency we observed both the walking stick phenotype and the branchiostegal-opercle transformation phenotype (Fig. 10). As indicated by the absence of joints between the palatoquadrate and Meckel's cartilage (Fig. 10, *), only partial rescue was obtained in both cases, suggesting that [Edn1] was lower than in the wild type.

## DISCUSSION

The bone phenotypes resulting from lowering Edn1 show that this signaling molecule plays a prominent role in bone patterning in the two anterior pharyngeal arches, as we previously recognised for pharyngeal cartilages (reviewed by Kimmel et al., 2001b). The variety of bone phenotypes include complete losses, partial reductions, expansions, fusions and shape changes. Such variations reveal complexity in Edn1's control of development of the exquisite patterning of early bone phenotype. Our data strongly suggest that the phenotype depends, at least in part, on how much the Edn1 signal is compromised.

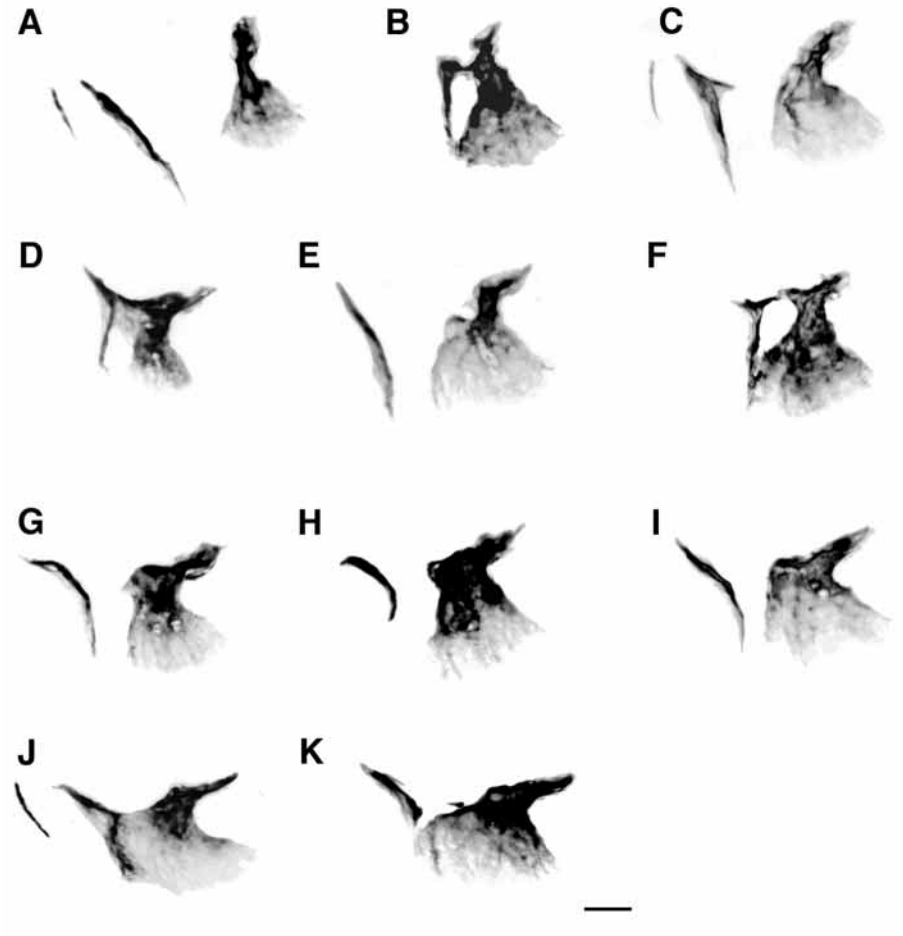


**Fig. 8.** Phenotypic series of opercle-gain and branchiostegal phenotypes in larvae with mild reductions of Edn1. Left-side views (confocal projections, Calcein labeling) with dorsal to the top at 6 or 7 days postfertilization. (A) Wild type (WT). (B-K) Mutants and MO-injected larvae arranged according to the extent of the increase in size of the opercle. (B,F) *she* mutants. (C) *edn1*-MO injected at 5 ng. (E,H,I,K) *edn1*-MO injected at 1.5 ng. (D,G,J) *stu* mutants. Two branchiostegal rays are present in (A) and (C), and apparently also in (J), in which the larger dorsal one is deformed and fused with the opercle by a thin but continuous sheet of bone. We interpret (K) as a similar prominent fusion between the disrupted branchiostegal ray and the opercle. (B,D,F) Examples of 'walking stick' phenotypes, showing fusions at the joint regions of the bones. (C) The branchiostegal ray is deformed with a spur appearing to correspond to an expanded joint region, also present in the walking stick examples. The fusions seem to occur all along the series (i.e. in examples with either a mild or severe opercle gain), whereas the curvature of the branchiostegal ray roughly increases along the series with the most extreme case in H. Scale bar: 50 μm.

## Dermal bone fusions in the mandibular and hyoid arches

The two anterior pharyngeal arches, mandibular and hyoid, are understood to be serially homologous pharyngeal segments, supported by the role of Edn1 in specifying DV pattern in both (reviewed by Kimmel et al., 2001a). Among the phenotypes caused by lowering Edn1 are fusions between ventral and dorsal cartilages in both arches. The dermal bone phenotypes extend this evidence: we suggest that both the 'wicket' phenotype in the mandibular arch and the 'walking stick' phenotype in the hyoid arch represent abnormal fusions between dorsal and ventral dermal bones, reminiscent of the DV cartilage fusions. However, there are interesting differences. The cartilages that fuse normally articulate with one another; the fusions represent missing joints. This is true for neither of the bone fusions. Whereas the DV cartilage fusions occur with mild Edn1 loss in both arches (Miller and Kimmel, 2001), dermal bone fusions resulting from mild Edn1 loss occur only in the hyoid arch, not in the mandibular arch. Furthermore, the way the bone wicket follows the line of the lips in the mandibular arch has no counterpart in the hyoid arch. Grafting studies have suggested a role of the oral epithelium

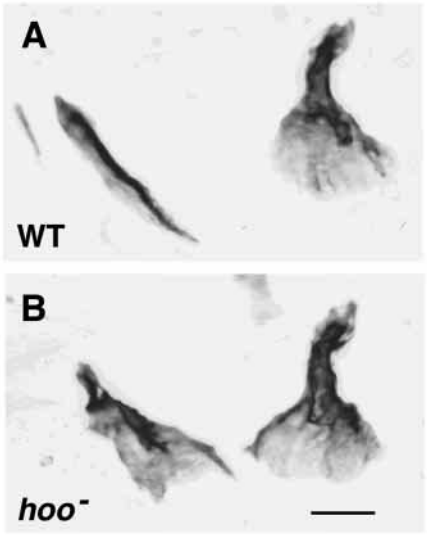


**Fig. 9.** Putative homeotic transformation of the dorsal branchiostegal ray towards the opercle in a *hoover* mutant. (A) A wild-type (WT) *hoo*$^{b631}$ sibling, showing the opercle and two branchiostegal rays, the more anterior one much smaller. (B) A *hoo* mutant. The opercle (right) is approximately normal in size and shape, but the bone at the usual position of the dorsal branchiostegal ray (left) has the form of an opercle. Its proximal end (upper) is sculptured into a distinctive joint region, rather than just ending bluntly as in A. Here DIC imaging (not shown; as in Fig. 4) reveals that the transformed branchiostegal ray makes a prominent joint with the underlying ceratohyal cartilage. Its distal region, normally blade-shaped, is expanded into an opercle-like fan. The other (more anterior and smaller) branchiostegal ray is missing. Scale bar: 50 μm.

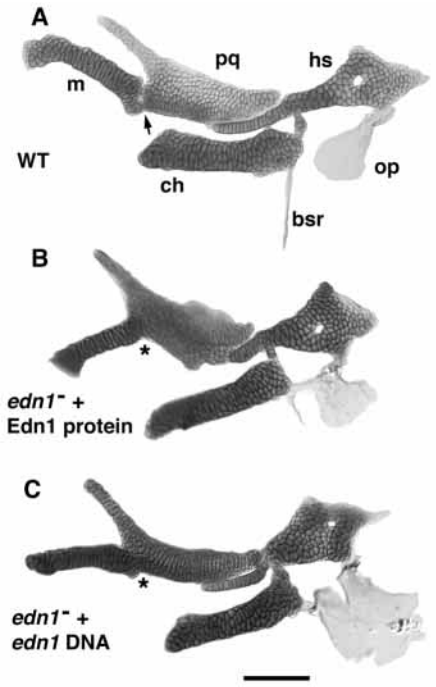


**Fig. 10.** Hyoid cartilage and bone in wild type (WT; A) and partially rescued *edn1* mutants (B,C). Left-side views with dorsal to the top and anterior to the left. (B) Walking stick fusion phenotype (similar to that of *stu* mutant in Fig. 8D) in an *edn1* mutant partially rescued by injecting human EDN1 protein. (C) Branchiostegal-opercle transformation phenotype (similar to that of the *hoo* mutant in Fig. 9B, but here the fan regions are fused) in an *edn1* mutant partially rescued adding back a zebrafish *edn1*$^{+}$ DNA construct. We have never observed either of these bone phenotypes in non-rescued *edn1* mutants. The methods of rescue are as described by Miller et al. (Miller et al., 2000). Rescue of the cartilage phenotype is only partial, as indicated by the absence of the joints in the mandibular arch (asterisk in B and C, the arrow indicates the normal joint in A). The cartilages and attached bones were dissected from the heads of fixed and Alcian Green-stained larvae 4 days postfertilization, and are shown as flat mounts. In vivo, the bones project more posteriorly away from the cartilages than shown in the dissected wild-type preparation. bsr, (posterior) branchiostegal ray; ch, ceratohyal cartilage; hs, hyosymplectic cartilage; m, Meckel's cartilage; op, opercle; pq, palatoquadrate cartilage. Scale bar: 50 μm.

in skeletal patterning in the chick (Tyler and Hall, 1977). Similarly, in zebrafish the lip epithelium may be involved in patterning mandibular dermal bone in a way that is not mirrored in the hyoid arch.

## A morphogen gradient model of bone patterning

Our loss of function analyses strongly suggest that the hyoid arch bone phenotype is exquisitely sensitive to the level of the *edn1* gene product, a secreted peptide. The findings extend previous understanding of *edn1* function derived from analyses of pharyngeal cartilages. The gene is expressed segmentally by ventrally located arch epithelia and mesoderm in the embryonic pharyngeal walls (Miller et al., 2000). The Edn1 peptide is secreted, such that it can serve as an extracellular signal acting on postmigratory skeletogenic neural crest cells. As a consequence, these cells transcriptionally upregulate target genes, such as the bHLH transcription factor-encoding gene *hand2*. In *edn1* mutants and in other anterior arch mutants the ventral cartilages are variably reduced and misoriented (Piotrowski et al., 1996; Kimmel et al., 1998). As shown previously (Miller and Kimmel, 2001) and also by this work, more severe ventral cartilage reductions correlate with more severe loss of Edn1, implying a developmental role of signal strength.

In common among all of the anterior arch mutants is the loss of joints between the dorsal and ventral cartilages of the first two pharyngeal arches, resulting in cartilage fusions. Edn1 appears to pattern joint development in a domain that lies either entirely or mostly more dorsal and not contiguous with the ventral signal source in the embryonic pharyngeal walls (Miller et al., 2003). This geometry also implies a role of signal strength, for we suppose that a ventral signal locally patterns crest cells to make ventral cartilage, and represses cartilage formation in slightly more dorsal cells, such that they make a joint rather than cartilage. In this model, the ventral cells respond to a higher level of the signal than the more dorsal ones.

Our new findings also support a model in which the bone phenotype depends not only on the amount of signal released, but also on the DV position within an arch of the responding cells. For example, extreme reduction of Edn1, as in injections of the highest levels of the *edn1*-MO, usually leads to the complete loss of both the ventral and dorsal bones in the hyoid arch (the ventral branchiostegal rays and the dorsal opercle). With only moderate loss of signal, the dorsal bone frequently persists and indeed, is enlarged, but ventral branchiostegal rays are usually missing. With mildest reduction of Edn1, both ventral and dorsal bones persist – although their shapes and sizes are abnormal. Dorsal structures respond to a ventral signal, suggesting that the signal acts at a location remote from its source. Ventral structures are more sensitive than dorsal ones to reduced signal, suggesting that higher levels of signal normally pattern the ventral bones and lower levels pattern the dorsal ones. These findings are consistent with the hypothesis that Edn1 functions as a morphogen in pharyngeal skeletal development: diffusion (or transport) of the peptide away from its ventral source sets up a concentration gradient to which the postmigratory neural crest cells differentially respond according to their DV positions in the arches. Fig. 11 depicts how the gradient model works to explain normal DV positioning of the branchiostegal ray and opercle (A), and how lowering the gradient to a more moderate level predicts both loss of the ventral bone and expansion of the dorsal one (B). Lowering the gradient still further predicts the observed loss of both bones (not shown).

The gradient model makes a prediction that we do not observe; namely loss of DV joints between cartilages in the anterior arches is more sensitive to Edn1 reduction than is loss of more ventral cartilage. By the model just outlined we expect the opposite, the more ventral tissue should be the more sensitive one (just as we observe for hyoid bone development). To explain this discrepancy, one can postulate that DV joint *position* is determined by an Edn1 gradient, but that joint *differentiation* requires additional Edn1-sensitive factors.

A morphogen gradient hypothesis provides a simple explanation for much of the phenotypic variation we observe, yet many factors must determine the cellular response to the

gradient. For example, the hyoid dermal bone fusions, the formation of joints by branchiostegal rays, and, in *hoo* mutants, branchiostegal ray shape transformation toward opercle (ventral toward dorsal), suggests that Edn1 is playing some role not only in positioning where bone develops, but also in specifying the character or 'identity' of the bone. Reduced signal can be interpreted by ventral bone-forming cells (in the sense of the French Flag model of Wolpert) (Wolpert, 1971) to mean that they are developing at a dorsal position – more remote from a ventral source, hence accounting for the transformation toward the shape of the dorsal bone.

## Patterning how much bone develops: negative regulation and the opercle-gain phenotype

Development of the opercle depends on Edn1, as revealed by its loss when the signal is severely lowered. In contrast, in the opercle-gain phenotype, a dramatically enlarged opercle develops. By the morphogen hypothesis it is the gradient of Edn1 in the arch that determines the mutant phenotype (i.e. the level at the ventral source and the slope, as in Fig. 11). An alternative scenario, that the signal is expressed locally to the bone, is suggested by studies in the mouse showing Edn1 expression within bone-forming primordia (Sasaki and Hong, 1993; Kitano et al., 1998). However, this explanation seems unlikely in zebrafish: the only arch mesenchyme in which we have observed *edn1* RNA expression is ventral mesoderm, and although our fate mapping of the embryonic pharyngeal arches is preliminary, the opercle appears to arise from postmigratory neural crest located dorsally in the arch primordia, distant from the Edn1 source (J. G. C., unpublished observations). Hence, in zebrafish the dermal bone primordia may not express the gene. Furthermore, we observed that the severities of both the cartilage and lateral line neuromast phenotypes correlate with the severities of opercle phenotypes (gain versus loss) in the same hyoid arch. These correlations might not be expected if only local expression of the *edn1* gene within the bone primordia determined the bone phenotype.

Correlated bone-cartilage and bone-neuromast phenotypes might also be indicating the presence of patterning interactions between these tissues, even if an Edn1 gradient is providing the positional information for where these interactions occur. The correlations are strong but they are not absolute, which might argue against local tissue interaction. Nevertheless, it is reasonable to suppose that interactions occur between the two tissues contributing to a joint, such as the hyosymplectic cartilage and the opercle bone. Ablation or transplantation experiments could reveal such interactions. Interactions between neuromasts and underlying dermal bone have been postulated for many years; e.g. in positioning lateral line canals that run through dermal bones (Allis, 1889; Parrington, 1948; Webb, 1989). Mutations are available that block zebrafish neuromast development (Whitfield et al., 1996), but it is not known if hyoid bones are affected in these mutants.

Regardless of the patterning mechanism, a key finding from our study is that with reduction of the Edn1 signal the size of the opercle expands, meaning that Edn1 negatively regulates dermal bone size. A role of Edn1 as a negative upstream regulator in zebrafish was previously suggested (Piotrowski et al., 1996), from an observation that dorsal cartilages are expanded in the loss of function *edn1* mutant. A more recent example is in muscle patterning. Dorsal muscles in the mandibular arch specifically express an Engrailed homeobox gene, *eng2*. In *edn1* mutants the *eng2* expression domain is expanded ventrally, showing that the ventral signal directly or indirectly is functioning as a repressor, and probably at some distance from its source (Miller et al., 2003).

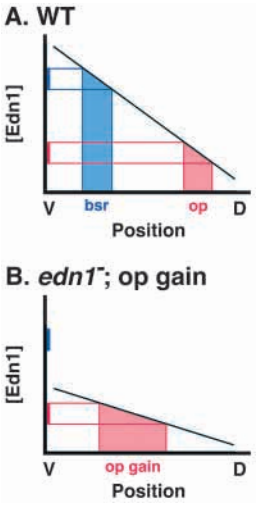


**Fig. 11.** A morphogen gradient model accounts for (A) the dorsal-ventral (DV) positioning of the branchiostegal ray (bsr) and opercle (op) of the wild type (WT), and (B) the combined loss of the branchiostegal ray and enlargement of the opercle typical of the *edn1* mutant opercle-gain phenotype (e.g. as in Figs 2 and 4). The model was suggested in part from a gradient model of neural crest specification by BMP (Nguyen et al., 1998). The source of the Edn1 gradient is ventral, as we infer from the *edn1* mRNA expression pattern in the ventralmost region of the developing pharyngeal arches (Miller et al., 2000; Miller et al., 2003). The sets of positional values (Wolpert, 1971) specifying the branchiostegal ray and opercle are shown along the Y axis in blue and red, respectively. (A) The bones are made in the local zones determined by these values, the branchiostegal ray is ventral to the opercle. (B) Lowering the Edn1 source decreases the slope of the gradient; positional values for the branchiostegal ray are now missing, resulting in loss of the ray, and the region of opercle specification expands, resulting in the opercle-gain phenotype. The model predicts that the enlarged opercle is present more ventrally in the hyoid arch than normal – closer to the Edn1 source. In fact, the position of the opercle seems not to be moved ventrally, rather the ventral part of the arch is missing or reduced in the mutant (Miller et al., 2000), such that the opercle would indeed be closer to a ventral gradient source. If the gradient is lowered more severely (not shown) then the positional values for the opercle would be missing as well, accounting for the opercle-loss phenotype.

## Hyoid dermal bone evolution and homeosis

Negative regulation is a well-known phenomenon in developmental genetics, but is generally not considered in discussions of how evolution of development works. Mutation toward loss of function is of course much more probable than mutation toward gain of function, and when the mutated gene is a negative regulator, the loss of function mutation results in an expanded rather than a reduced phenotype, here with respect to bone size. More bone comes from less genetic function, and this certainly has important implications for evolutionary change.

The highly specialized dermal bone pattern in the zebrafish hyoid arch might derive evolutionarily from a long DV series of uniform branchiostegal ray-like elements (McAllister, 1968) (Fig. 1). Changes in Edn1 regulation might underlie the evolutionary changes. We discovered that Edn1 negatively regulates the size of the opercle, the dorsal-most element of the branchiostegal-opercle series in zebrafish. Hence a ventral to dorsal gradient of Edn1 accounts for a dorsal to ventral gradient of bone size that apparently evolved in early osteichthyans. The evolving opercle would have gained new muscle attachments

and a more efficient hinged joint. We observed that when Edn1 is mildly reduced the opercle-gain phenotype includes ectopic muscle attachments (Fig. 4), that a branchiostegal ray can develop a joint region resembling that of the opercle and develop the opercle's fan shape. Finally, when Edn1 is severely reduced (as in *edn1* mutants), branchiostegal rays are absent, correlating with the evolutionary loss of branchiostegal rays that occurred in parallel in several teleost lineages (McAllister, 1968). Of the two branchiostegal rays generally developing in the young wild-type larvae, the more ventral one ($bsr_m$, closer to the putative signal source) is almost never present in mutants. Therefore, Edn1 positively regulates formation of branchiostegal rays, and possibly in a concentration- and position-dependent manner. Evolution of a lower number of them may also have involved changes in Edn1 level or in the sensitivities of the responding cells.

We interpret the branchiostegal-opercle transformation as homeosis; dissimilar meristic elements become similar (Bateson, 1894). Hubbs (Hubbs, 1920) previously placed the branchiostegal rays and opercle into a single meristic series, which is in accord with a hypothesis of homeotic change between the elements. However, there are caveats concerning our interpretation. We do not have specific genetic markers for bone identity that we can use to test for homeosis. Furthermore, even if the transformation is indeed one of bone identity, and can be induced by just manipulating the level of Edn1 (as suggested by the rescue experiments in Fig. 10), it is important to note that *hoo* might be playing other roles in skeletal patterning than its putative role in the Edn1 signaling pathway. Similar to *she* and *stu*, the molecular nature of the *hoo* gene has not yet been described. Furthermore, the low penetrance of the transformation phenotype (expansion of the branchiostegal ray occurs in only 4% of *hoo* mutants) clearly indicates that unknown factors (other than the proposed Edn1 gradient) are playing critical roles in specifying bone identity.

Homeosis is well-known along the anterior-posterior axis of the embryo. The transformations are between segmental homologs. The homeotic genes are usually either *Hox* genes or genes that interact with *Hox* genes. In contrast, the axis of patterning along the hyoid arch is the DV axis, and there is no well-understood role of *Hox* genes in DV pharyngeal patterning (but see Davenne et al., 1999). Other candidates are available: *Dlx* homeobox genes regulate DV patterning differences (maxillary versus mandibular) in the mammalian first arch (Depew et al., 2002) (reviewed by Panganiban and Rubenstein, 2002), and members of the TGFβ superfamily regulate the formation of molars versus incisors along the mammalian jaw bones (Tucker et al., 1998; Ferguson et al., 2001). *Msx* homeobox genes regulate bone development (e.g. Dodig et al., 1999), including a negative regulation of bone size through interaction with the osteoblast-specifying homeobox gene *Runx2* (Shirakabe et al., 2001). *Msx* and *Dlx* genes, targets of Edn1 signaling in the zebrafish pharyngeal arches (Miller et al., 2000), also control bone matrix development by reciprocal regulation of Osteocalcin, a bone matrix protein (Newberry et al., 1998). Learning the nature of target genes controlled by Edn1 in the zebrafish hyoid arch that cell-autonomously control dermal bone size and DV identity would be a fruitful avenue for future work.

We thank Paula Mabee, Judith Eisen and Monte Westerfield for discussion and comments on earlier versions of the manuscript. Research support was provided by NIH grants DE13834 and HD22486.

## REFERENCES

**Allis, E. P.** (1889). The anatomy and development of the lateral line system in *Amia calva*. *J. Morphol.* **2**, 463-567.

**Bateson, W.** (1894). *Materials for the Study of Variation.* London: Macmillan & Co.

**Beresford, W. A.** (1996). Cranial skeletal tissues: diversity and evolutionary trends. In *The Skull*, vol. 2 (ed. J. Hanken and B. K. Hall), pp. 69-130. Chicago and London: The University of Chicago Press.

**Carroll, R. L.** (1988). *Vertebrate Paleontology and Evolution*. New York: W. H. Freeman.

**Charité, J., McFadden, D. G., Merlo, G., Levi, G., Clouthier, D. E., Yanagisawa, M., Richardson, J. A. and Olson, E. N.** (2001). Role of Dlx6 in regulation of an endothelin-1-dependent, *dHAND* branchial arch enhancer. *Genes Dev.* **15**, 3039-3049.

**Clouthier, D. E., Hosoda, K., Richardson, J. A., Williams, S. C., Yanagisawa, H., Kuwaki, T., Kumada, M., Hammer, R. E. and Yanagisawa, M.** (1998). Cranial and cardiac neural crest defects in endothelin-A receptor-deficient mice. *Development* **125**, 813-824.

**Clouthier, D. E., Williams, S. C., Yanagisawa, H. Wieduwilt, M., Richardson, J. A. and Yanigisawa, M.** (2000). Signaling pathways crucial for craniofacial development revealed by endothelin-A receptor-deficient mice. *Dev. Biol.* **217**, 10-24.

**Cubbage, C. C. and Mabee, P. M.** (1996). Development of the cranium and paired fins in the zebrafish *Danio rerio* (Ostariophysi, cyprinidae). *J. Morphol.* **229**, 121-160.

**Davenne, M., Maconochie, M. K., Neun, R., Pattyn, A., Chambon, P., Krumlauf, R. and Rijli, F. M.** (1999). Hoxa2 and Hoxb2 control dorsoventral patterns of neuronal development in the rostral hindbrain. *Neuron* **22**, 677-691.

**Depew, M. J., Lufkin, T. and Rubenstein, J. L. R.** (2002). Specification of jaw subdivisions by *Dlx* genes. *Science* **298**, 381-385.

**Dodig, M., Tadic, T., Kronenberg, M. S., Dacic, S., Liu, Y. H., Maxson, R., Rowe, D. W. and Lichtler, A. C.** (1999). Ectopic Msx2 overexpression inhibits and Msx2 antisense stimulates calvarial osteoblast differentiation. *Dev. Biol.* **209**, 298-307.

**Ferguson, C. A., Tucker, A. S., Heikinheimo, K., Nomura, M., Oh, P., Li, E. and Sharpe, P. T.** (2001). The role of effectors of the activin signalling pathway, activin receptors IIA and IIB, and Smad2, in patterning of tooth development. *Development* **128**, 4605-4613.

**Hubbs, C. L.** (1920). A comparative study of the bones forming the opercular series of fishes. *J. Morphol.* **33**, 61-71.

**Hubbs, C. L. and Hubbs, L. C.** (1945). Bilateral asymmetry and bilateral variation in fishes. *Papers of the Michigan Academy of Sciences, Arts and Letters* **30**, 229-310.

**Janvier, P.** (1996). *Early Vertebrates*. Oxford: Clarendon Press.

**Jarvik, E.** (1980). *Basic Structure and Evolution of Vertebrates*. London, New York, Toronto, Sydney, San Francisco: Academic Press.

**Johnson, S. L. and Weston, J. A.** (1995). Temperature-sensitive mutations that cause stage-specific defects in zebrafish fin regeneration. *Genetics* **141**, 1583-1595.

**Jollie, M.** (1962). *Chordate Morphology*. New York: Rheinhold.

**Kempf, H., Linares, C., Corvol, P. and Gasc, J.-M.** (1998). Pharmacological inactivation of the endothelin type A receptor in the early chick embryo: a model of mispatterning of the branchial arch derivatives. *Development* **125**, 4931-4941.

**Kimmel, C. B., Miller, C. T. and Keynes, R. J.** (2001a). Neural crest patterning and the evolution of the jaw. *J. Anat.* **199**, 105-119.

**Kimmel, C. B., Miller, C. T., Kruse, G., Ullmann, B., BreMiller, R. A., Larison, K. D. and Snyder, H. C.** (1998). The shaping of pharyngeal cartilages during early development of the zebrafish. *Dev. Biol.* **203**, 245-263.

**Kimmel, C. B., Miller, C. T. and Moens, C. B.** (2001b). Specification and morphogenesis of the zebrafish larval head skeleton. *Dev. Biol.* **233**, 239-257.

**Kitano, Y., Kurihara, H., Kurihara, Y., Maemura, K., Ryo, Y., Yazaki, Y. and Harii, K.** (1998). Gene expression of bone matrix proteins and

endothelin receptors in endothelin-1-deficient mice revealed by in situ hybridization. *J. Bone Miner. Res.* **13**, 237-244.

**Kurihara, Y., Kurihara, H., Suzuki, H., Kodama, T., Maemura, K., Nagal, R., Oda, H., Kuwaki, T., Cao, W.-H., Kamada, N. et al.** (1994). Elevated blood pressure and craniofacial abnormalities in mice deficient in endothelin-1. *Nature* **368**, 703-710.

**Maisey, J. G.** (1986). Heads and tails: a chordate phylogeny. *Cladistics* **2**, 201-256.

**Maves, L., Jackman, W. and Kimmel, C. B.** (2002). FGF3 and FGF8 mediate a rhombomere 4 signaling activity in zebrafish hindbrain. *Development* **129**, 3825-3837.

**McAllister, D. E.** (1968). The evolution of branchiostegals and associated opercular, gular, and hyoid bones. *Bull. Natl. Mus. Canada* **221**, 1-239.

**Miles, R. S.** (1973). Articulated acanthodian fishes from the Old Red Sandstone of England, with a review of the structure and evolution of the acanthodian shoulder-girdle. *Bull. Br. Mus. Nat. His. Geol.* **24**, 115-213.

**Miller, C. T. and Kimmel, C. B.** (2001). Morpholino phenocopies of endothelin 1 (*sucker*) and other anterior arch class mutations. *Genesis* **30**, 186-187.

**Miller, C. T., Schilling, T. F., Lee, K.-H., Parker, J. and Kimmel, C. B.** (2000). *sucker* encodes a zebrafish Endothelin-1 required for ventral pharyngeal arch development. *Development* **127**, 3825-3828.

**Miller, C. T., Yelon, D., Stainier, D. Y. R, and Kimmel, C. B.** (2003). Two *endothelin 1* effectors, *hand2* and *bapx1*, pattern ventral pharyngeal cartilage and the jaw joint. *Development* **130**, 1353-1365.

**Nelson, G. J.** (1970). The hyobranchial apparatus of teleostean fishes of the families Engraulidae and Chirocentridae. *Am. Mus. Nov.* **2410**, 1-30.

**Newberry, E. P., Latifi, T. and Towler, D. A.** (1998). Reciprocal regulation of osteocalcin transcription by the homeodomain proteins Msx2 and Dlx5. *Biochemistry* **37**, 16360-16368.

**Nquyen, V. H., Schmid, B., Trout, J., Connors, S. A., Ekker, M. and Mullins, M. C.** (2003). Ventral and lateral regions of the zebrafish gastrula, including the neural crest progenitors, are established by a *bmp2b/swirl* pathway of genes. *Dev. Biol.* **199**, 93-110.

**Panganiban, G. and Rubenstein, J. L.** (2002). Developmental functions of the *Distal-less*/*Dlx* homeobox genes. *Development* **129**, 4372-4386.

**Parenti, L. R.** (1986). The phylogenetic significance of bone types in euteleost fishes. *Zool. J. Linnean Soc.* **87**, 37-51.

**Parrington, F. R.** (1948). A theory of the relations of lateral lines to dermal bones. *Proc. Zool. Soc. Lond.* **119**, 65-78.

**Piotrowski, T., Schilling, T. F., Brand, M., Jiang, Y. J., Heisenberg, C. P., Beuchle, D., Grandel, H., Van Eeden, F. J. M., Furutani-Seiki, M., Granato, M. et al. (**1996). Jaw and branchial arch mutants in zebrafish. 2. Anterior arches and cartilage differentiation. *Development* **123**, 345-356.

**Raible, D. W. and Kruse, G. J.** (2000). Organization of the lateral line system in embryonic zebrafish. *J. Comp. Neurol.* **421**, 189-198.

**Russell, E. S.** (1916). *Form and Function: a Contribution to the History of Animal Morphology*. London: J. Murray.

**Sasaki, T. and Hong M. H.** (1993). Endothelin-1 localization in bone cells and vascular endothelial cells in rat bone marrow. *Anat. Rec.* **237**, 332-337.

**Schultze, H.-P.** (1993). Patterns of diversity in the skulls of jawed fishes. In *The Skull*, Vol. 2 (ed. J. Hanken and B. K. Hall), pp. 189-254. Chicago and London: The University of Chicago Press.

**Shirakabe, K., Terasawa, K., Miyama, K., Shibuya, H. and Nishida, E.** (2001). Regulation of the activity of the transcription factor Runx2 by two homeobox proteins, Msx2 and Dlx5. *Genes Cells* **6**, 851-856.

**Thomas, T., Kurihara, H., Yamagishi, H., Kurihara, Y., Yazaki, Y., Olson, E. N. and Srivastava, D.** (1998). A signaling cascade involving endothelin-1, dHAND and Msx1 regulates development of neural-crest-derived branchial arch mesenchyme. *Development* **125**, 3005-3014.

**Tucker, A. S., Matthews, K. L. and Sharpe, P. T.** (1998). Transformation of tooth type induced by inhibition of BMP signaling. *Science* **282**, 1136-1138.

**Tyler, M. S. and Hall, B. K.** (1977). Epithelial influences on skeletogenesis in the mandible of the embryonic chick. *Anat. Rec.* **188**, 229-240.

**Verraes, W.** (1977). Postembryonic ontogeny and functional anatomy of the ligamentum mandibulo-hyoideum and the ligamentum interoperculo-mandibulare, with notes on the opercular bones and some other cranial elements in *Salmo gairdneri* Richardson, 1836 (Teleostei: Salmonidae). *J. Morphol.* **151**, 111-120.

**Webb, J. F.** (1989). Developmental constraints and evolution of the lateral line system in teleost fishes. In *The Mechanosensory Lateral Line* (ed. S. Coombs, P. Görner and H. Münz), pp. 79-97. New York: Springer-Verlag.

**Whitfield, T. T., Granato, M., Van Eeden, F. J. M., Schach, U., Brand, M., Furutani-Seiki, M., Haffter, P., Hammerschmidt, M., Heisenberg, C. P., Jiang, Y. J. et al. (**1996). Mutations affecting development of the zebrafish inner ear and lateral line. *Development* **123**, 241-254.

**Wolpert, L.** (1971). Positional information and pattern formation. *Curr. Top. Dev. Biol.* **6**, 183-224.

**Yanagisawa, H., Yanagisawa, M., Kapur, R. P., Richardson, J. A., Williams, S. C., Clouthier, D. E., de Wit, D., Emoto, N. and Hammer, R. E.** (1998). Dual genetic pathways of endothelin-mediated intercellular signaling revealed by targeted disruption of endothelin converting enzyme-1 gene. *Development* **125**, 825-836.